Construction and Building Materials 295 (2021) 123686

Contents lists available at ScienceDirect

Construction and Building Materials

journal homepage: www.elsevier.com/locate/conbuildmat

Phosphorus removal enhancement by porous adsorptive mortar using miscanthus and steel slag for highly adsorptive concrete

Fan Wu [a,b], Qingliang Yu [b,c,*], H.J.H. Brouwers [b]

[a] Key Laboratory of Mountain Hazards and Earth Surface Process, Institute of Mountain Hazards and Environment, Chinese Academy of Sciences, No.9 Section 4, Renmin South Road, Chengdu 610041, PR China
[b] Department of the Built Environment, Eindhoven University of Technology, P.O. Box 513, 5600 MB Eindhoven, the Netherlands
[c] School of Civil Engineering, Wuhan University, No.299 Bayi Road, Wuchang District, Wuhan 430072, PR China

HIGHLIGHTS

- Porous adsorptive mortar is designed and developed for improving P-removal.
- Heat-treated miscanthus improves P-adsorption capacity of mortar-coated aggregate.
- The adsorption capacity of the adsorptive mortar is 30.4–74.2 mg/g.
- Adsorption mechanism is analyzed by ICP-AES, XRD, FTIR, TG-DTG and SEM-EDS.

GRAPHICAL ABSTRACT

Schematic diagram of the adsorption process and mechanism of aggregates coated with porous adsorptive mortar for P-removal.

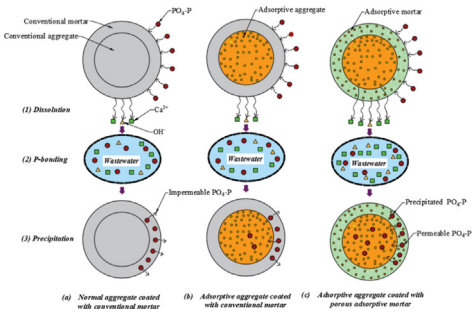

ARTICLE INFO

Article history:
Received 4 April 2021
Received in revised form 16 May 2021
Accepted 17 May 2021

Keywords:
Miscanthus
Steel slag
Phosphorus removal
Adsorptive mortar
Highly adsorption concrete

ABSTRACT

The low permeability and low adsorption capacity of conventional cement mortar are one of the decisive reasons for the poor adsorption performance of the adsorptive aggregates applied to adsorptive concrete. In this study, a porous adsorptive mortar is developed by combining chemical and physical methods to enhance the permeability and adsorption performance. Porous heat-treated miscanthus (HM) (0.5 wt% and 1.0 wt%) powder and steel slag (SS) (5.0 wt% and 10.0 wt%) powder with different dosages are investigated in this new adsorptive mortar. Results show that the excellent adsorption capacity of the adsorptive mortar of 30.4–74.2 mg/g, with a corresponding initial P-concentration of 1215.3–2967.5 mg/L. The leaching result, ICP-AES, XRD, FTIR, TG-DTG and SEM-EDS analyses confirm the Ca^{2+} leached from the adsorptive mortar and the SS, reacting with the PO_4^{3-} to form Ca-P precipitates in solution. Moreover, the porous HM significantly improves the permeability of the developed mortar. It is can be concluded that the HM with a dosage of 0.5 wt% and the SS with a dosage of 10.0 wt% can be recommended for highly adsorptive mortar to improve phosphorus (P) removal capacity from stormwater, without obvious sacrifices on other properties.

1. Introduction

The rapid development of civilization results in an increasing impact on the aquatic environment [1]. The urban surface, such

* Corresponding author at: Department of the Built Environment, Eindhoven University of Technology, P.O. Box 513, 5600 MB Eindhoven, the Netherlands
E-mail address: q.yu@bwk.tue.nl (Q. Yu).

https://doi.org/10.1016/j.conbuildmat.2021.123686
0950-0618/

as street, parking lot, roof, etc. is usually considered as a critical source area for the production of contaminants [2,3]. In the rainy season, stormwater runoff carries various contaminants including phosphorus (P), nitrogen, heavy metals, etc. generated by urban surface directly into the nearby water body, increasing the pollution degree of water body. Among these contaminants, P is the main element that causes algae bloom and eutrophication [3,4]. Once the concentration of P in water body exceeds 0.03 mg/L, the algae and aquatic plant will experience an accelerated growth with an abnormal rate, reducing the quality of the water body [4]. Previous studies show 75–90% of P that is transported with stormwater runoff is in the particulate form [5]. Therefore, the P-removal from stormwater runoff is of great significance for reducing water pollutants and improving water quality during the transfer of pollutants with the stormwater runoff.

Considering the reduction of contaminants from stormwater runoff during pollutant solution passing through pervious concrete, the adsorption characteristics of ordinary porous pervious concrete have begun to attract more and more attention recently. Previous studies have shown that in the process of rainwater infiltration, porous pervious concrete can adsorb water pollutants, such as P [6], heavy metals (Mn, Co and Ni, etc.) [7], and fecal coliforms [8]. However, the current pervious concrete usually has a low adsorption capacity and needs a very long reaction time for pollutant removal from stormwater runoff. Vázquez-Rivera et al. [6] investigated the P-adsorption capacity of pervious concrete containing iron oxide and fly ash with an initial P-concentration of 10 mg/L, indicating that P-removal is attributed to the Ca^{2+} leached from mortar bonds with PO_4^{3-} to precipitate in forms of hydroxyapatite ($Ca_{10}(PO_4)_6(OH)_2$) and amorphous calcium phosphate ($Ca_3(PO_4)_2$). Shabalala et al. [7] reported that the pervious concrete successfully removes more than 75% of heavy metals, but 6 months are needed for the Ca^{2+} to react with SO_4^{2-} for sulphate removal. Jot et al. [8] reported that the pervious concrete containing fly ash can remove fecal coliforms and P, and the P-removal rate is 25–85%, with an initial P-concentration of 2.58–3.4 mg/L. Okano et al. [9] investigated that the P-removal capacity of the autoclaved lightweight concrete particles is only 6–10%, while amorphous calcium silicate hydrate can remove approximately 69–73% of the P from wastewater with an initial P-concentration of 89 mg/L. It is concluded that porous pervious concrete can be used for pollution removal, but the removal rate of current pervious concrete is very low. More importantly, a long reaction time and a low initial concentration of the pollutant are required. Therefore, the adsorption performance of pervious concrete should be improved prior to application for the P-removal from stormwater runoff.

Previous studies have shown that industrial by-products such as steel slag (SS) [10], blast furnace slag [11], fly ash [12] and lightweight sludge particle [13], etc. can be used in water treatment for P-removal from wastewater. Agyei et al. [12] reported that the P adsorption capacity of cement, SS, and fly ash are 83 mg/g, 60 mg/g and 32 mg/g, respectively, and the removal efficiency and capacity of P-removal depend on the percentage of CaO and the amount of Ca^{2+} ion released into solution by dissolution and hydration. One of the main components of SS is calcium oxide [14], and usually the calcium-containing mineral exceeds 50% [15], indicating that sufficient Ca^{2+} can be provided by SS for calcium-phosphorus precipitation [16]. Besides, SS can participate in the hydration of cement [17–19] and can be potentially used to replace cement to reduce the negative impact of cement on the environment, such as high carbon footprint [20]. More importantly, our previous study has confirmed that the heavy metals (As, Co, Cr, Mn, Se, V, etc.) leached from the SS are well below the limit values for building materials [21]. Therefore, SS can be used as sustainable building materials potentially to improve the adsorption characteristics of adsorptive mortar by increasing chemical adsorption.

The adsorption capacity of porous adsorptive materials usually depends on the microstructure and pore characteristics [22]. In particular, the increase in well-developed micropores (<2 nm) and specific surface area can improve the adsorption capacity of adsorptive materials by physical method [23]. Miscanthus (M) is a leading perennial energy grass in Europe [24], which has gained an increasing attention for the manufacture of bio-based lightweight concrete [25]. Compared to normal weight concrete, bio-based miscanthus concrete has lightweight characteristics and associated better thermal and sound insulation, attributed to the developed micropores [26]. Furthermore, considering the sustainability and environmental friendliness of the adsorptive mortar, the M is renewable and possesses great potential in saving natural materials and decreasing the cost of building materials. Therefore, the porous M may be used to improve the micropores of the adsorptive mortar and promote the penetration of pollutants into the mortar layer that will be then absorbed by the adsorptive aggregate for improving the pollutant removal capacity.

P-removal mechanism is generally based on chemical reactions between metal cations (e.g. Ca^{2+}, Fe^{3+} and Al^{3+}) and the phosphate anion species (HPO_4^{2-} and PO_4^{3-}) [9]. Among these cations, Ca^{2+} is the main reactive ion with phosphate anion species, which can be available for P recovery [27]. The driving mechanism during the adsorption process of P-crystallization consists essentially of nucleation by precipitation of hydroxyapatite ($Ca_{10}(PO_4)_6(OH)_2$) [28]. However, crushed rock (basalt, limestone, etc.) is usually used as coarse aggregates in ordinary pervious concrete. But the lack of adsorption ability of crushed rock results in a poor adsorption performance of ordinary pervious concrete. The adsorption capacity is only attributed to the reaction of mortar and P in the solution. The adsorption performance of potentially adsorptive aggregates is analyzed in our previous work [29], the predicted P-adsorption capacities of SS and heat-treated M by Langmuir isotherm model are 20.4 mg/g and 3.68 mg/g, respectively. It is hypothesized that the replacement of normal weight aggregate without any adsorption capacity by highly adsorptive aggregates will significantly enhance the adsorption capacity of porous adsorptive concrete.

The manufacture of a highly adsorptive aggregate made from the SS and the heat-treated M with physical and chemical adsorption is reported in our previous work [21]. Similar to normal weight aggregates, when highly adsorptive aggregates are applied to the concrete matrix, its surface will be coated with normal mortar. The P-removal potential of adsorptive aggregate particles is generally controlled by its permeability, which is related to the ability to release Ca^{2+} into solution. Highly dense mortar layer will significantly reduce the penetration potential of pollutants into the adsorptive aggregate, resulting in a significant reduction in the adsorption performance. Therefore, a porous permeable mortar is developed in this study to improve the adsorption performance of mortar-coated aggregates.

In order to improve the adsorption performance of the adsorptive concrete, a porous permeable mortar with good permeability and adsorption is proposed in this study. The chemical method by adding adsorptive materials (SS) and the physical method by adding porous materials (heat-treated miscanthus (HM)) are used to increase the adsorption capacity of the cement mortar. Firstly, the effects of the SS and the HM powder on cement hydration are analyzed by a TAM air isothermal calorimeter. Then the physical, mechanical properties and adsorption characteristics of adsorptive mortar are investigated. Moreover, the effects of the adsorptive mortar on the adsorption capacity of the aggregate are also analyzed. The leaching test results (ICP-AES), mineralogical phase (XRD), microstructure (SEM-EDS) infrared spectra (FTIR) and thermal gravimetric results (TGA-DTG) of adsorptive mortar before

and after adsorption test are analyzed for the understanding of adsorption mechanism.

2. Materials and methods

2.1. Materials

Miscanthus (M) powder (Vibers, The Netherlands) and converter steel slag (SS) powder (TATA Steel, The Netherlands) are used as porous materials and adsorption materials, respectively, to improve the permeability and adsorption characteristics of the adsorptive mortar in the present study, as shown in Fig. 1. Portland CEM I 52.5 R cement is used as the binder, provided by ENCI (The Netherlands). The raw M is heat-treated for 3 h at a temperature of 250 ℃ under nitrogen gas to increase its adsorption characteristics by increasing the microporous structure [29]. The specific density of the heat-treated miscanthus (HM) and the SS is 1.25 g/cm^3 and 3.9 g/cm^3, respectively. The 24-h water absorption of the HM is 350 ± 21%. The BET specific surface areas of the HM and the SS are 5.14 m^2/g and 1.98 m^2/g, respectively. The chemical composition of the cement and the SS are determined by X-ray fluorescence, as shown in Table 1.

The microscopic images of the HM and the SS are analyzed using a scanning electron microscope (SEM) (Phenom ProX). As presented in Fig. 1, many longitudinal bundle-like micropores exist inside the stalk of the HM, which can significantly improve the porosity and permeability of cement paste. The surface of the SS is a dense structure with some microscopic cracks.

The mineralogical phases of the HM and the SS are determined by X-ray diffraction (XRD) (Bruker AXS) analysis, as given in Fig. 2. The M is mainly a plant fibre composed of C, H and O elements [30], therefore only an obvious diffraction peak is observed at the diffraction angle of about 25° due to the presence of crystalline cellulose. The main mineral components of the SS are 3CaO·SiO$_2$ (C$_3$S), 2CaO·SiO$_2$ (C$_2$S) and RO (Fe$_2$O$_3$, MgO and MnO) [31]. These metal mineral components, especially calcium-containing crystal components, contribute to P-removal from wastewater [29,32].

2.2. Preparation of adsorptive mortar

The schematic diagram of the improvement of permeability and adsorption performance of cement mortar is shown in Fig. 3. When the adsorptive aggregate is coated by conventional mortar, it is difficult for pollutants to reach the highly adsorptive aggregate or only a small amount of pollutants could penetrate the adsorptive aggregate due to the low permeability of normal mortar. In order to improve the permeability of the mortar-coated aggregates, the HM is adopted in the present study to form porous structure inside the mortar for the improvement of adsorption performance by physical method. When the permeability of the mortar is increased by the HM, more pollutants can penetrate the paste, and then contact with the adsorptive aggregate, and subsequently be absorbed by the highly adsorptive aggregate. The SS is applied as an adsorbent material to improve the P-adsorption capacity of the adsorptive mortar by chemical method. The P from pollutants can be absorbed by the SS during the pollutants pass through the adsorptive mortar process [21].

A paste containing 400 kg/m^3 cement and 200 kg/m^3 water is used as the control mix (C0) with a water to cement (W/C) of 0.5 referring to the preparation method of standard mortar (EN 196-1:2005). Due to high content of miscanthus [25] and steel slag [33] will significantly reduce the performance of mortar, the HM with a content of 0.5 wt% and 1 wt% of cement and the SS of 5 wt% and 10 wt% of cement are added to the other four batches of paste, which are labelled as HM0.5, HM1, SS5and SS10, respectively.

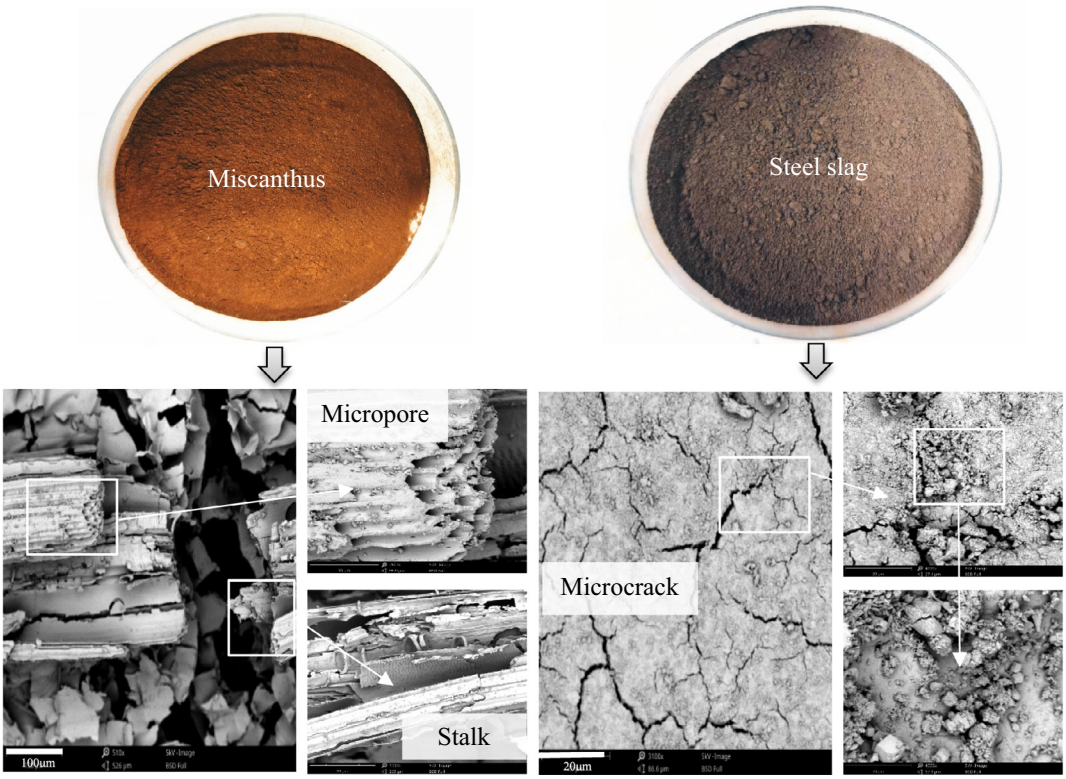

Fig. 1. Heat-treated miscanthus powder and steel slag powder and their microscopic images.

Table 1
Chemical composition of cement and steel slag (wt.%).

Oxides	CaO	SiO_2	Al_2O_3	Fe_2O_3	SO_3	MgO	K_2O	Na_2O	LOI
Cement	64.60	20.08	4.98	3.24	3.13	1.98	0.53	0.27	0.40
Steel slag	37.97	10.37	1.61	31.48	0.43	4.92	–	–	3.25

2.3. Effects of adsorptive mortar on adsorption performance of aggregates

When the adsorptive aggregate is coated with different types of paste, its adsorption characteristics will be affected by factors such as the permeability and adsorption capacity of the cement mortar. In order to investigate the effects of the mortar containing the M and the SS on the actual adsorption performance of the adsorptive aggregate, the previously manufactured adsorptive aggregates (SS75) with a size of 2–5 mm are applied in the present study. The adsorptive aggregate is produced through 75 wt% steel slag and 25 wt% lightweight expanded silica, which has high adsorption characteristics and good mechanical properties. The P-adsorption capacity and removal rate of the adsorptive aggregate are 4.2 mg/g and 100%, respectively, with an initial P-concentration of 168 mg/L. The detailed manufacturing process and characteristics of this adsorptive aggregate are shown in our previous research [21]. The properties of adsorptive aggregates are shown in Table 2.

The preparation process of coating aggregates with adsorptive mortar is presented in Fig. 4. Firstly, the adsorptive aggregate is poured into the prepared fresh paste (Fig. 4a, b), and then the adsorptive aggregate and the mortar is mixed until the adsorptive aggregate is evenly coated by the mortar (Fig. 4c). After that, the mortar on the surface of the aggregate is rounded manually, and the thickness of the mortar layer is controlled of about 0.5–1 mm (Fig. 4d). Finally, the aggregates coated with the mortar are stored in a standard curing room until the adsorption test.

2.4. Testing methods

2.4.1. Cement hydration test

Generally, bio-based materials have an adverse effect on cement hydration due to the presence of organic matter [34]. The influence of the M and the SS on the hydration characteristics of cement is measured using a TAM air isothermal calorimeter at the constant temperature of 20 ℃. The M and the SS are mixed with cement and water, respectively, with a water-cement ratio of 0.5. The percentage of the M mixed with cement is chosen as 0.5 wt% and 1 wt% of cement, the amount of the SS is 5 wt% and 10 wt% of cement, respectively. The mortar without any M and SS is used for the control mix (C0). After mixing, all samples are placed in the calorimeter to determine the hydration behavior of cement.

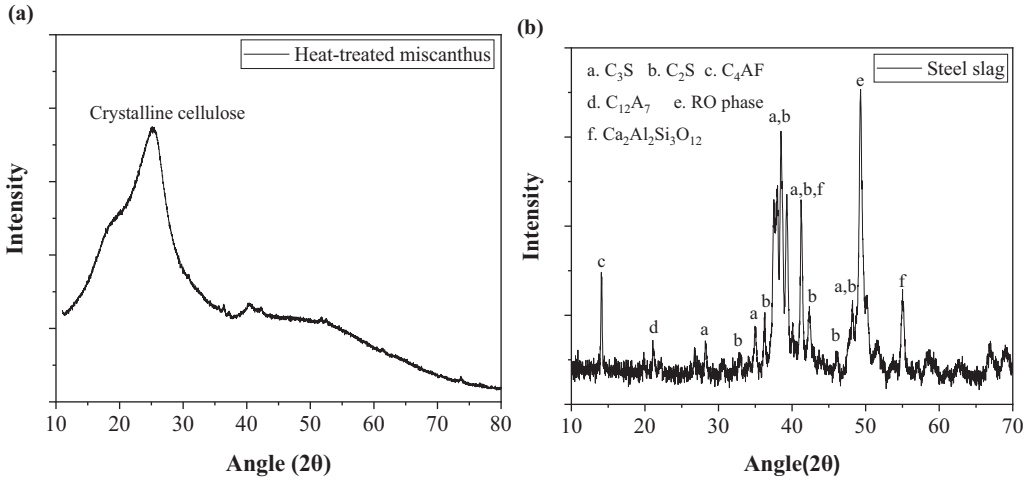

Fig. 2. X-ray diffraction of heat-treated miscanthus and steel slag.

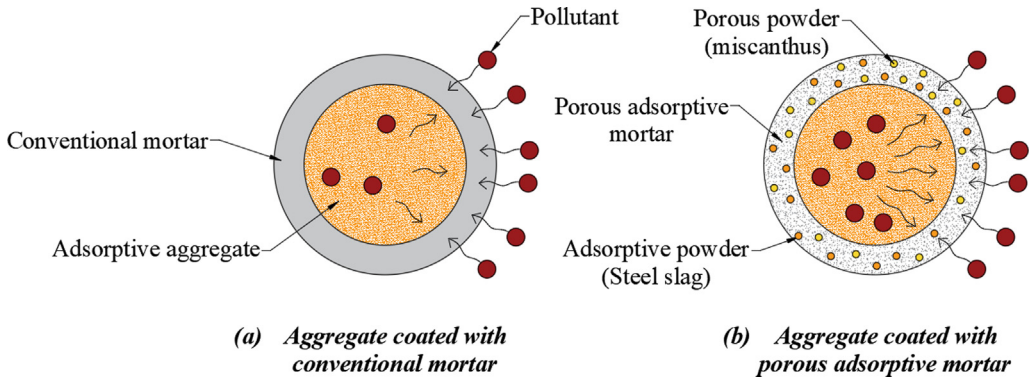

Fig. 3. Schematic diagram of the improvement of permeability and adsorption performance of adsorptive mortar.

Table 2
Properties of adsorptive aggregates (SS75).

Adsorptive aggregate	Size (mm)	Particle density (kg/m^3)	Bulk density (kg/m^3)	24-hour water absorption (%)	Crushing strength (MPa)
SS75	2–5	2633.3	882.5	12.7	5.13

2.4.2. Physical and mechanical test

The density, water absorption and porosity of all samples are determined according to ASTM C642-13. 40 × 40 × 40 mm^3 and 40 × 40 × 160 mm^3 samples with a curing age of 28 days are used for determining the compressive strength and flexural strength, respectively, according to EN 196–1. The constant loading rates of compressive strength and flexural strength test are 2400 N/s and 0.05 MPa/s, respectively. The average value of three samples is reported as the test result. The microscopic image of the sample is observed by a scanning electron microscope (SEM).

2.4.3. Adsorption test

Phosphorus (P) is one of the main pollutants in water pollution, leading to eutrophication of water bodies [35]. In this study, P is used to simulate the polluted water for the adsorption test. The current adsorption studies mainly focus on the low P-concentration adsorption test [16,29]. Because of the high adsorption characteristics of adsorptive aggregates, three high-concentration P solutions (1215.3 mg/L, 1849.3 mg/L and 2967.5 mg/L) are used for adsorptive mortar adsorption test and mortar-coated aggregate adsorption test in this study. Firstly, 1 g of adsorptive mortar (or mortar-coated adsorptive aggregate) is added to a small plastic bottle with 25 ml P solution. Secondly, the plastic bottle with adsorptive mortar and P solution is stirred at 225 rpm in the shaker for 24 h and then is filtered by a 0.45 μm membrane to obtain the extracted supernatant. The change in the P-concentration of the solution is determined using an ion chromatography (IC) analyzer (Thermo Dionex Aquion).

The P-adsorption capacity (q, mg/g) and P-removal rate (P_R, %) are calculated by:

$$q = \frac{C_0 - C_e}{M} \times V \quad (1)$$

$$P_R = \frac{C_0 - C_e}{C_0} \times 100\% \quad (2)$$

Where C_0 is the initial P concentration (mg/L), C_e is the P concentration in the solution after adsorption test (mg/L), M is the mass of sample (g), and V is the volume of solution (L).

To investigate the adsorption mechanism of adsorption mortar, ions leached from the adsorptive mortar are determined according to EN 12457–2. Firstly, adsorptive mortar and distilled water are mixed with a solid–liquid ratio of 10, i.e. 10 g adsorptive mortar is mixed with 100 ml of distilled water, and then shaken using a dynamic shaker with a speed of 250 rpm for 24 h. Finally, the leachates are filtered by a 0.22 μm filter and acidified with concentrated HNO_3 for the leaching test by inductively coupled plasma atomic emission spectroscopy (ICP-AES) (SPECTROBLUE). The mineralogical phase and microstructure of samples before and after adsorption test are measured by XRD and SEM-EDS, respectively, and the sample is further analyzed by Fourier transform infrared spectroscopy (FTIR) (PerkinElmer) and thermogravimetry (TG-DTG) (STA 449 F1 Jupiter) for better understanding of adsorption mechanism of adsorptive mortar.

3. Results and discussion

3.1. Hydration behavior of adsorptive mortar

The saccharides leached from the bio-based material such as hemp, coir, bagasse and oil palm shell, etc. have a negative effect on cement hydration [34]. The organic acids show strong calcium chelating groups that can reduce the concentration of Ca^{2+} and prevent the formation of calcium-silicate-hydrate (C-S-H) and portlandite [36], resulting in a decrease of mechanical strength, crystallinity and hydration of cement [34,37] and an increasing setting time [38].

In this study, the addition of 0.5 wt% and 1 wt% HM shows an insignificant influence on cement hydration (Fig. 5). At 80 h, the total released heat of HM0.5 and HM1 is only reduced by 0.2% and 1.8% (Table 4), respectively, compared to the control mortar (C0). This may be attributed to that heat treatment changes the biomass content (cellulose, hemicellulose and lignin) of the HM, and oxygen-containing saccharides are pyrolyzed and more carbon is formed during the pyrolysis process, which ultimately leads to a

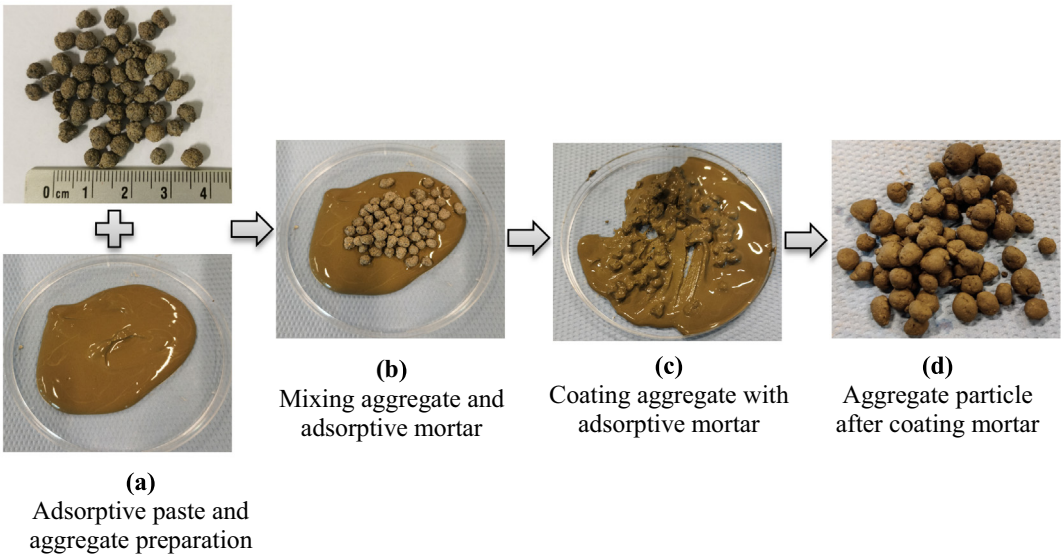

Fig. 4. Preparation process of coating adsorptive aggregates with adsorptive mortar.

lessened effect on cement hydration [30,39]. Boix et al. [36] reported that the alkali-treated miscanthus accelerates the hydration of cement compared to the untreated miscanthus, and a direct inverse relationship is found between the sugar content extracted from miscanthus and the mechanical strength of bio-based miscanthus concrete. Therefore, the HM is more advantageous to increase the porosity of adsorptive mortar while minimizing its negative impacts on the cement hydration and mechanical strength of adsorptive mortar.

As shown in Table 3, the addition of 5 wt% and 10 wt% SS reduces the total heat of cement hydration by 3.4% and 6.8%, respectively. The total released heat of cement hydration decreases with an increasing dosage of the SS, because the low calcium silicates content and the C_2S in the SS slow down the cement hydration [17]. Because the large-sized SS particles can not act as nucleation sites for the deposition and crystal growth of hydration products [18], thus the total heat and hydration rate are reduced with the increasing dosage of the SS. However, for the heat flow curve (Fig. 5b), no obvious delay is observed in the SS5 and SS10 curve. It is concluded that adding of the SS up to 10 wt% in this study does not significantly alter the hydration of cement.

3.2. Physical and mechanical properties of adsorptive mortar

3.2.1. Density, water absorption and porosity

The density of adsorptive mortar is shown in Fig. 6a. As expected, the addition of the HM slightly decreases the density of adsorptive mortar, while the SS significantly increases the density. The changes in oven-dry density of HM0.5, HM1, SS5 and SS10 are −2.1%, −3.1%, +3.4% and + 8.0%, respectively, compared to the control mortar (C0). These results are consistent with the previous studies [26,38], i.e. the addition of the bio-based miscanthus reduces the density of concrete due to its porosity and lightweight properties, the SS significantly increases the density of concrete structure [40].

Water absorption is a very important indicator of the adsorption performance of adsorptive concrete. High water absorption means that the pollutants can be quickly absorbed by adsorptive concrete, which is usually related to the amount and size of the micropores, as well as the connectivity. As shown in Fig. 6b, both the M and the SS increase the water absorption and permeable porosity of the adsorptive mortar. The water absorption of the HM0.5, HM1, SS5 and SS10 increases by 2.7%, 10.0%, 3.6% and 8.2%, respectively, and the corresponding permeable porosity increases by 6.0%, 13.3%, 4.0% and 10.0%, respectively, compared to the control mortar (C0). Due to the high porous structure of the HM, it can generally absorb several times water higher than its mass. The water absorption of the miscanthus is related to the particle size and the 48-hour water absorption of 2–4 mm, 0–2 mm and powdery miscanthus is about 290%, 400% and 525%, respectively, reported by Chen et al. [26]. Therefore, the HM is a practical bio-based material that can be used to improve the permeability of the adsorptive mortar for a better pollutant removal capacity.

Table 3
Released heat comparison of adsorptive mortar (80 h).

Items	C0	HM0.5	HM1	SS5	SS10
Total heat (J/g)	241.0	240.6	236.6	232.7	224.6
Heat deviation (J/g)	–	−0.4	−4.4	−8.3	−16.4
Reduction (%)	–	0.2	1.8	3.4	6.8

3.2.2. Compressive strength and flexural strength

The mechanical properties of adsorptive mortar are the decisive factors of the mechanical strength of adsorptive concrete. The compressive strength and flexural strength of adsorptive mortar are shown in Fig. 7. The results show that the M reduces the compressive strength of adsorptive mortar and the SS does not significantly affect the compressive strength. Moreover, the mechanical strength of the adsorptive mortar decreases with an increasing dosage of the M and the SS. This may be because the addition of the M and the SS increase the porosity of the adsorptive mortar, resulting in a decrease in mechanical strength. The 28-day compressive strengths of the HM0.5, HM1, SS5 and SS10 are 59.7 MPa, 57.8 MPa, 63.2 MPa and 60.5 MPa, respectively.

Generally, the addition of waste has a significant impact on the mechanical properties of concrete [41,42]. The addition of bio-based materials significantly reduces the mechanical strength of concrete because of the low strength, high porosity and organic matter of bio-based materials [43]. The same phenomenon is observed in bio-based lightweight concrete, such as miscanthus concrete [26], oil palm shell concrete [44], apricot shell concrete [10], and wood concrete [45]. However, the heat-treated bio-based material has better dimensional stability and less organic content, resulting in a positive effect on the mechanical strength of concrete compared to untreated bio-based materials [46].

The results also show that the addition of the M and the SS results in a more significant reduction in flexural strength than compressive strength. The 28-day flexural strengths of the HM0.5, HM1, SS5 and SS10 are 2.89 MPa, 1.99 MPa, 3.20 MPa and 2.65 MPa, respectively. The decrease in mechanical strength is mainly because the addition of the M and the SS reduces cement hydration of the mortar. Based on the results, a high content of the

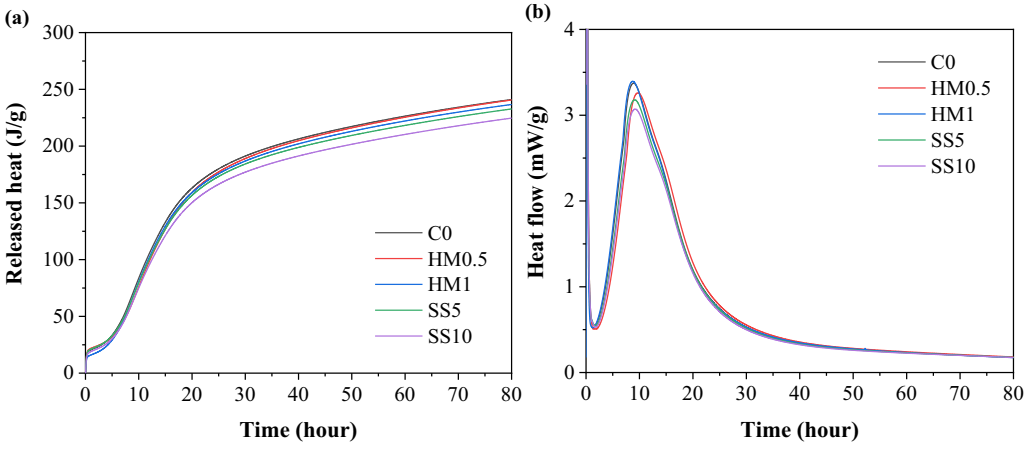

Fig. 5. Effects of miscanthus and steel slag powders on (a) released heat and (b) heat flow of cement hydration.

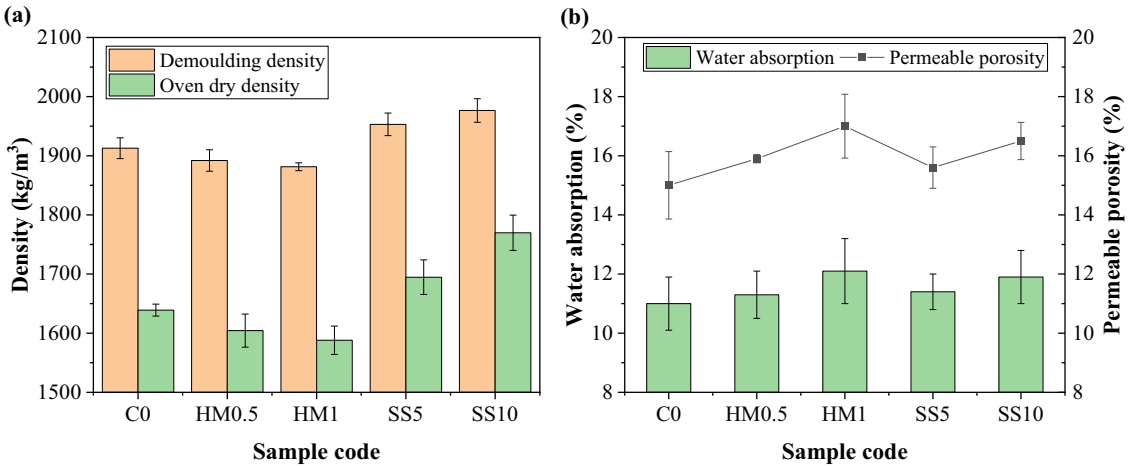

Fig. 6. (a) Density and (b) water absorption and permeable porosity of adsorptive mortar.

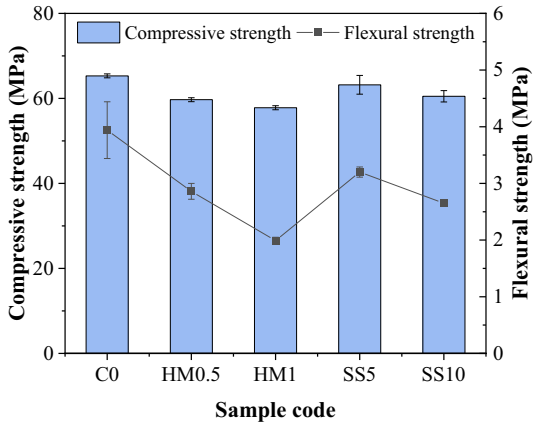

Fig. 7. Compressive and flexural strengths of adsorptive mortar at the age of 28 days.

HM powder (e.g. more than 1.0 wt%) is not recommended for adsorptive mortar due to the significant decrease in mechanical strength.

3.2.3. Microstructure

The SEM micrographs of adsorptive mortar (HM1 and SS10) are shown in Fig. 8. Micropores are observed on the surface of the HM1 and the SS10 sample. Moreover, the surface of the M and the SS does not closely bond with the mortar interface, and obvious microcracks exist in the interfacial transition zone. The same phenomenon has also been reported in bio-based lightweight concrete such as oil palm shell concrete [47], wood sand concrete [48] and bamboo reinforced concrete [49]. These microcracks and micropores increase the water absorption of the adsorptive mortar, increasing the easiness for the pollutants to penetrate the mortar layer. However, these microcracks are also one of the primary reasons for the mechanical strength reduction of the adsorptive mortar. Enough transport channels for the number of cracks are also observed on the HM surface because of the increase in brittleness of the HM after heat treatment. Luo et al. [50] reported that the average pore size of the miscanthus after heat treatment at 300 °C is 1.03 μm, which can provide a physical adsorption. Heat treatment not only reduces the pore size of the HM but also increases its specific surface area and ion exchange capacity. Therefore, the well-developed micropores and high specific surface area of the HM after pyrolysis endow it with an adsorption capacity for pollutant removal from wastewater [29].

3.3. Adsorption performance of adsorptive mortar

3.3.1. Adsorption capacity

The results show that no phosphorus (P) is detected in the solution after the adsorption test, except for the HM0.5 under a high initial P-concentration of 2697.5 mg/L condition, which indicates that the P is completely removed by the adsorptive mortar even at a high initial P-concentration. The P-adsorption capacity of the adsorptive materials depends on the initial concentration of the P solution [29]. When the initial P-concentration is 1215.3 mg/L, 1849.3 mg/L and 2967.5 mg/L, the adsorption capacity of the most adsorptive mortars (except for HM0.5) is 30.4 mg/g, 46.2 mg/g and 74.2 mg/g, respectively. The excellent adsorption capacity of the adsorptive mortar is attributed to the Ca^{2+} leached from the SS and mortar, which can react with the PO_4^{3-} to form Ca-P precipitates [18]. Besides, the porous miscanthus can also adsorb P through physical adsorption [29] and increase the permeability of the adsorptive mortar, which helps the leaching of Ca^{2+} from the adsorptive mortar surface.

The adsorption capacity of different materials for P-removal is presented in Table 4. The results show that the adsorption capacity of the developed adsorptive mortar is significantly higher than most of the adsorptive materials, including industrial by-products, natural material and bio-based material. More importantly, other adsorptive materials usually focus on the P-removal with a low P-concentration (i.e. <1000 mg/L). The adsorptive mortar in this study completely removes all P from P-solution with a high concentration of up to 2967.5 mg/L, showing an outstanding adsorption capacity. Therefore, it can be concluded that the developed adsorptive mortar can be applied to significantly improve the P-adsorption performance of porous adsorptive concrete.

3.3.2. Adsorption mechanism of adsorptive mortar

The adsorption of materials can generally be divided into physical adsorption and chemical adsorption. The adsorption of adsorptive mortar for P-removal is mainly dominated by chemical adsorption supplied by the mortar and the SS. The microporous structure formed by the HM also contributes to physical adsorption by pore-filling and electrostatic attraction [58]. P-removal rate by hydroxyapatite crystallization is usually affected by pH, temperature and concentration of PO_4^{3-} and Ca^{2+} [9]. The Ca^{2+}, K^+ and Na^+ ions are the main ions leached from the adsorptive mortar. The Ca^{2+} ion has a strong affinity with P, whereas other metal ions such as K^+, Na^+ and Mg^{2+} ions do not significantly affect the P-adsorption capacity [59,60]. The hydration products of mortar are mainly

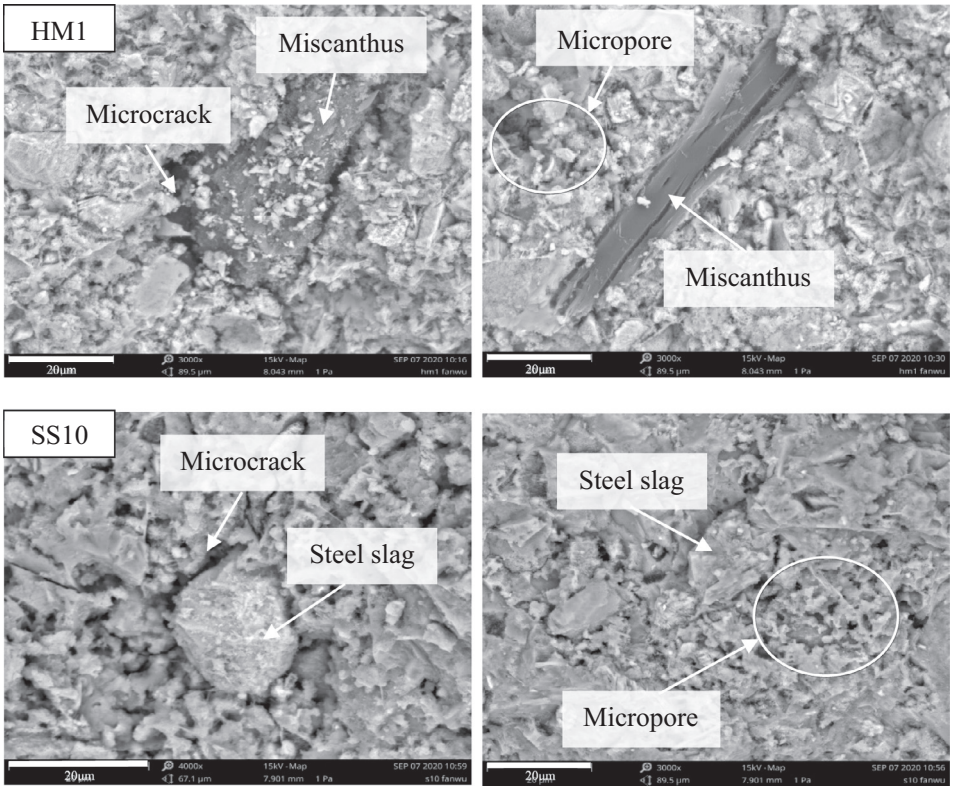

Fig. 8. SEM micrographs of adsorptive mortar.

Table 4
Adsorption capacity of different materials for P-removal.

Type	Materials	Initial concentration (mg/L)	Contact time (h)	Adsorption capacity (mg/g)	P-removal rate (%)	Reference
Concrete	Adsorptive mortar	1215.3–2967.5	24	30.4–74.2	100	In this study
	Portland cement	400	–	83	–	Agyei et al. [12]
	Quartz sand	25	24	0.3	87.7	Han et al. [51]
	Fly ash concrete	2.58–3.4	0.5–8	–	25–85	Jo et al. [8]
	Pervious concrete	10	72	–	>90	Vázquez-Rivera et al. [6]
Industrial by-product	Steel slag	700	24	9.76	55	Wu et al. [29]
	Furnace slag	–	24	2.81	–	Park et al. [52]
	Fly ash	400	16	32	–	Agyei et al. [12]
	Coal ash	35–45	12	0.86	–	Drizo et al. [53]
Natural material	Sepiolite	100	24	32	86	Yin et al. [35]
	Palygorskite	1000	24	42	–	Gan et al. [54]
Bio-based material	Peanut shell	5	48	3.8	61.3	Jung et al. [55]
	Miscanthus	50	24	0.12–0.22	8–14.7	Wu et al. [29]
	Bamboo	6.5	24	<2.5	42.15	Ramola et al. [56]
	Juniper fiber	10	24	<0.5	–	Han et al. [57]

Table 5
Chemical compositions of adsorptive mortar before and after adsorption (wt.%).

Oxides	C0		HM0.5		HM1		SS5		SS10	
	Before	After	Before	After	Before	After	Before	After	Before	After
CaO	60.94	60.85	60.61	60.01	60.82	59.79	59.32	58.97	57.55	55.07
SiO_2	15.95	15.94	15.86	15.48	15.92	15.38	15.63	15.33	15.26	14.31
Al_2O_3	6.72	6.79	7.06	7.03	6.92	7.09	6.71	6.52	6.76	6.75
Fe_2O_3	3.60	3.62	3.59	3.55	3.62	3.69	5.07	5.28	6.27	6.27
SO_3	2.80	2.76	2.77	2.63	2.76	2.60	2.51	2.48	2.42	2.21
MgO	1.39	1.34	1.38	1.29	1.38	1.23	1.70	1.61	1.91	1.71
P_2O_5	–	–	–	0.07	–	0.50	–	0.55	–	–

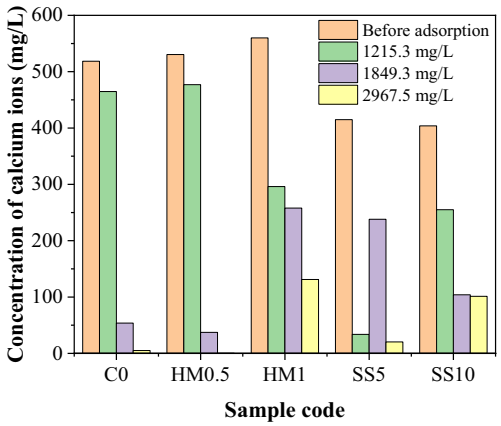

Fig. 9. Changes in the concentration of calcium ion released from adsorptive mortar in the solution.

hydrated calcium silicate and calcium hydroxide. Therefore, the Ca^{2+} ion leached from the mortar and the SS is one of the main ions for P-adsorption of adsorptive mortar.

The chemical compositions of adsorptive mortar before and after adsorption are presented in Table 5. The results showed that the content of calcium oxide (CaO) is slightly reduced after the adsorption test, which indicates that it participates in the reaction of Ca-P precipitation. In addition, P_2O_5 is found in the HM0.5, HM1 and SS5, which proves that P has a chemical reaction with the adsorptive mortar. The changes in the concentration of Ca^{2+} ion released from adsorptive mortar in the solution are shown in Fig. 9. The concentration of the Ca^{2+} ion after adsorption decreases in different P-solutions (1215.3 mg/L, 1849.3 mg/L and 2967.5 mg/L), compared to the initial concentration of the Ca^{2+} before absorption. Therefore, the adsorptive mortar containing high calcium content has a high P-adsorption capacity.

3.3.3. Mineralogical phase analysis

The XRD patterns are not significantly different before and after adsorption for all adsorptive mortars, taking sample SS5 as an example for explanation, as shown in Fig. 10a. Previous studies show that the direct reaction between the SS and cement is not obvious from this work or has a low reaction degree by RO phase and Fe_2O_3 [61]. The adsorptive mortar is mainly composed of calcium hydroxide ($Ca(OH)_2$) and modified alite phases ($Ca_{54}MgAl_2Si_{16}O_{90}$) before adsorption [62]. High concentration P-solution (1215.3 mg/L, 1849.3 mg/L and 2967.5 mg/L) is a weak acidic solution with a pH value of 4.64–4.83. After adsorption test, calcium aluminum sulfate hydroxide known as sulfate ettringite ($Ca_6Al_2(SO_4)_3(OH)_{12}\cdot 26H_2O$) (AFt) is observed at the diffraction angles of

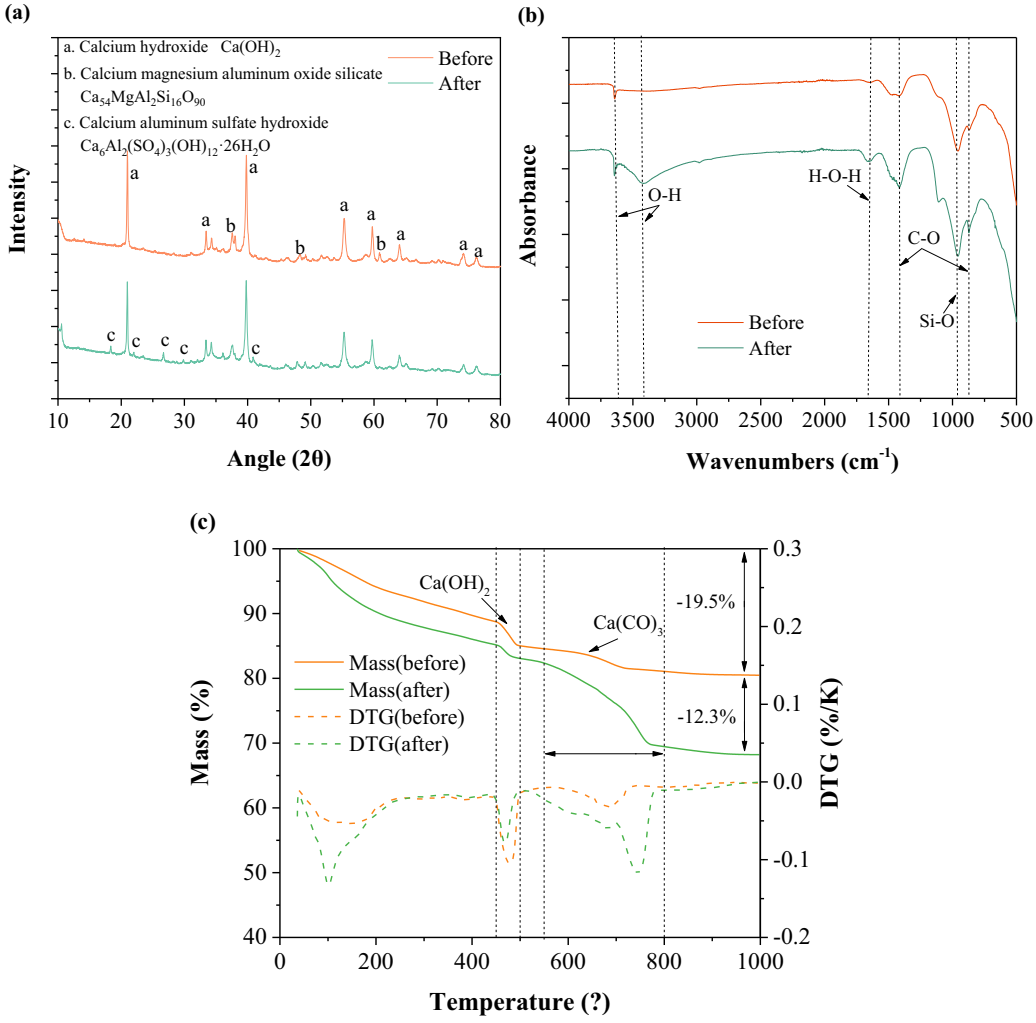

Fig. 10. (a) XRD patterns, (b) Infrared spectra and (c) TG-DTG of the SS5 before and after adsorption.

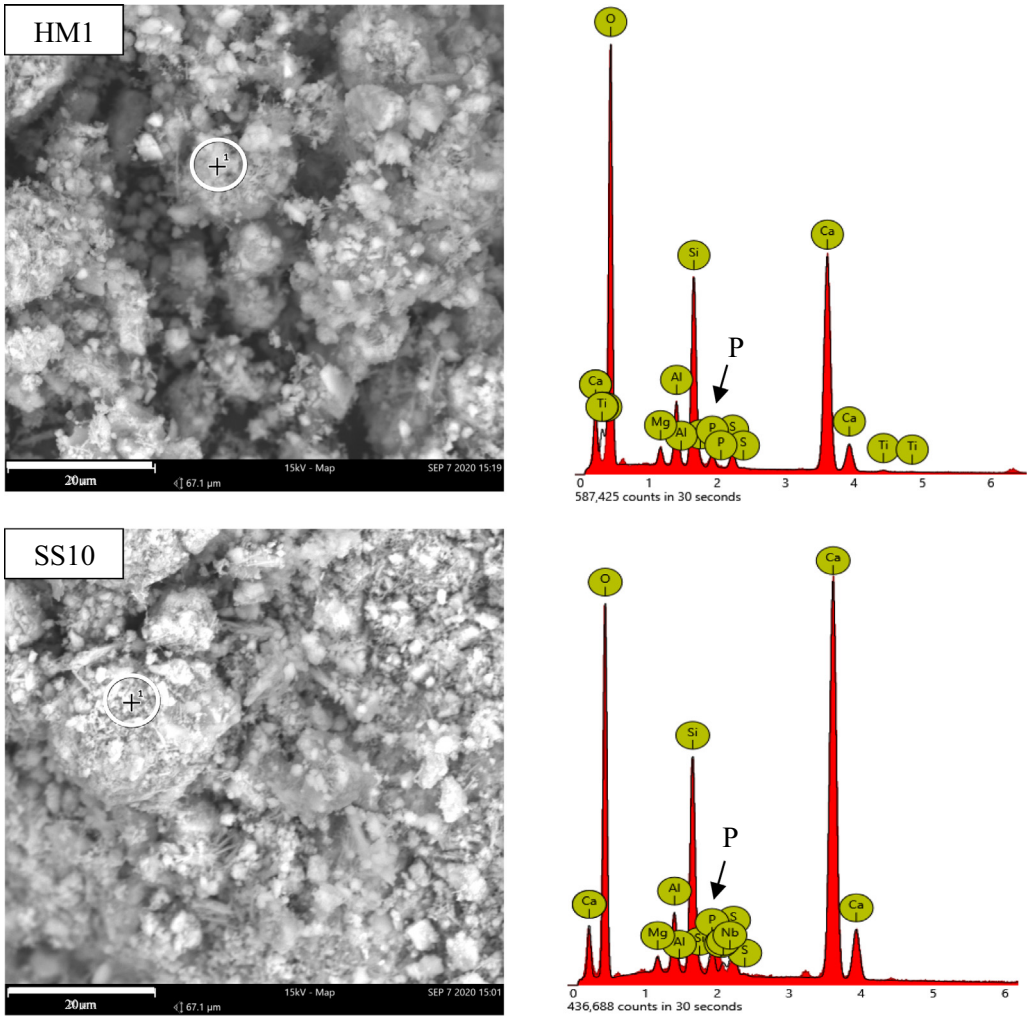

Fig. 11. SEM-EDS analysis of adsorptive mortar after adsorption.

18-30° and around 41°, which is usually formed in the early stages of cement hydration by calcium sulfate ($CaSO_4{\cdot}2H_2O$ and $CaSO_4{\cdot}0.5H_2O$) reacting with $Ca_3Al_2O_6$ (C_3A) at room temperature [63].

3.3.4. FTIR analysis

The infrared spectra of the SS5 before and after adsorption are presented in Fig. 10b. The spectrum presents an intense narrow band at 3635 cm^{-1}, which is a stretching vibration generated by the hydrogen bonds (O–H) bonds in portlandite ($Ca(OH)_2$) that is formed in the cement hydration [64]. The hydroxyl group with O–H bond usually appears at the wavelength of 3434 cm^{-1} due to symmetric and antisymmetric stretching vibration of water bounding from the hydrated products [65]. Moreover, an absorption band (H-O–H) at the wavelength of 1639 cm^{-1} shows deformation vibration of water molecules [19,66]. The adsorptive mortar after adsorption has an obvious peak at 3434 cm^{-1} and 1639 cm^{-1}, which may be due to the influence of the bound water in the sulfate ettringite ($Ca_6Al_2(SO_4)_3(OH)_{12}{\cdot}26H_2O$) (Aft phase). Furthermore, a narrow sharp band appears at 1112 cm^{-1}, which is associated with the stretching vibration of SO_4^{2-} group, supporting the presence of sulfate ettringite [67]. This result is consistent with the previous researches. The hydrated products of cement are typically characteristic by the Si-O asymmetric stretching vibration with a peak for the C-S-H at 970 cm^{-1} [68]. Calcium carbonate ($CaCO_3$) is originally present in mortar because of the chemical reaction between portlandite and atmospheric carbon dioxide (CO_2), resulting in C-O bending vibration and stretching with a peak appear at 713 cm^{-1}, 872 cm^{-1} and 1417 cm^{-1} [36,65,68].

3.3.5. TG-DTG analysis

The thermal gravimetric results of the SS5 are illustrated in Fig. 10c. Generally, a distinct mass loss for cementitious materials at a temperature of 130–200 ℃, 400–500 ℃ and 500–800 ℃, indicating the dehydration, the dihydroxylation or calcination of ettringite, the decomposition of $Ca(OH)_2$ and the decarbonation of $CaCO_3$, respectively [17]. The TG curves show that the all adsorptive mortars have a similar endothermic peak within 1000 ℃ before or after adsorption. The SS5 has a lower mass loss than C0 and HM0.5, indicating that fewer hydration products are generated due to the retardation of cement hydration by SS [17]. An endothermic peak appears at around 100 ℃ in the DTG curve related to the free moisture loss [69]. Besides, the dehydration of C-S-H appears below 200 ℃, which also matches with the weight loss description in mass loss curve [70,71]. A sharp decline of mass is observed at a temperature range of 450–500 ℃ for all adsorptive mortar, which is corresponding to the decomposition of crystalline $Ca(OH)_2$ [40,61]. The result is consistent with the XRD analysis. A significant mass loss is observed at the temperature of 550–800 ℃, which is related to the thermal decomposition

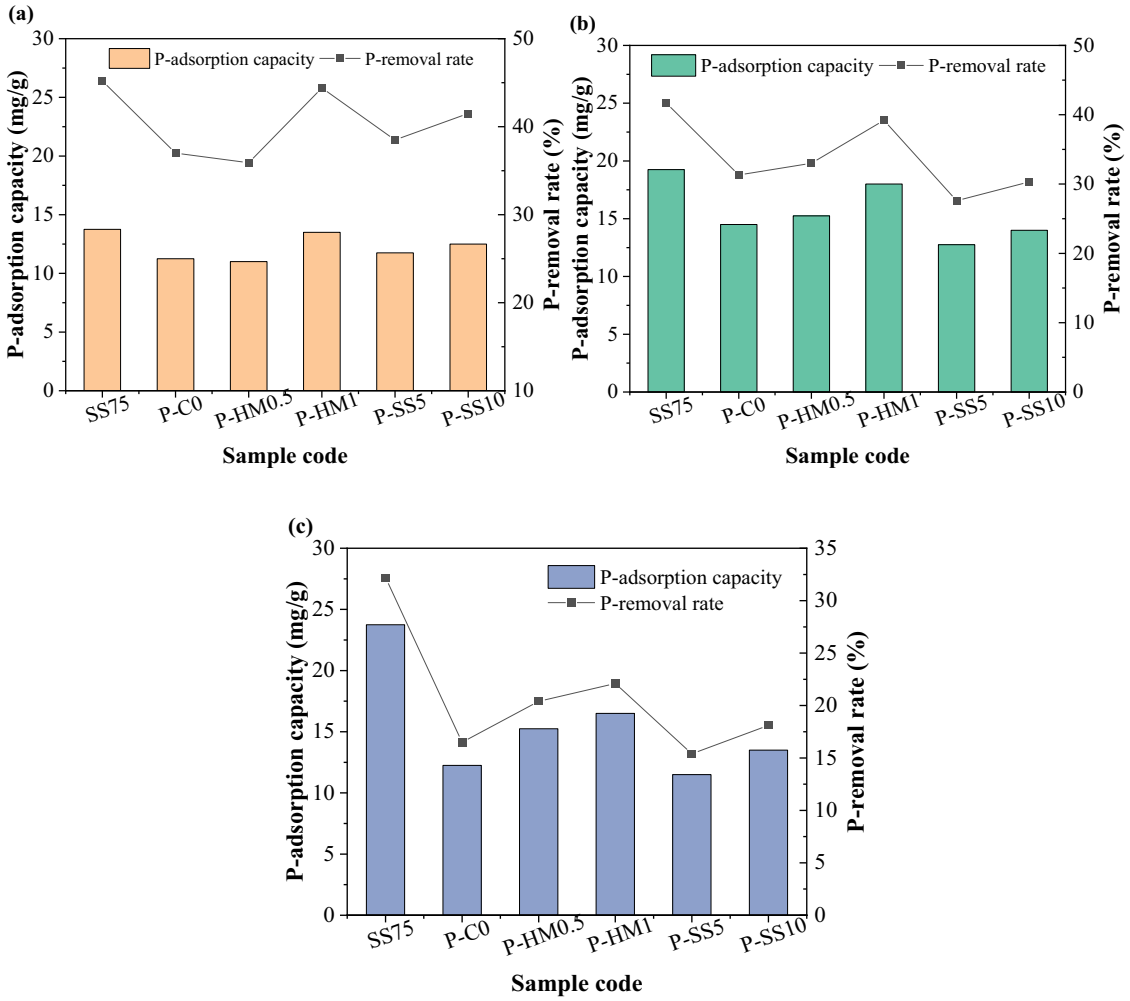

Fig. 12. P-adsorption capacity and removal rate of adsorptive aggregates with an initial P concentration (a) 1215.3 mg/L, (b) 1849.3 mg/L and (c) 2967.5 mg/L.

of $CaCO_3$ [72]. The result shows that the weight loss of the SS5 is lower than that of the C0 and HM0.5, indicating that the lower cement hydration product incorporating the SS. This result is consistent with the hydration heat result analysis as reported in section 3.1.

3.3.6. SEM-EDS analysis

The adsorptive mortar after adsorption is analyzed by SEM-EDS, as shown in Fig. 11, the C-S-H gel has a dense network structure, which indicates that enough hydration products are formed. Moreover, the crystallized needle-like ettringite is presented in micropores [17]. A strong peak of P appears in the EDS spectra and P is detected on the adsorptive mortar surface. Previous studies have reported that the small white crystalline substance on the surface is the suspended Ca-P precipitation [35,73]. The results also show that many micropores are observed on the surface of the HM1 and SS5. This may be due to the addition of the HM and the SS increases the porosity of the adsorptive mortar, causing more P-solution to penetrate the mortar layer and favor the combination with Ca^{2+} to form Ca-P precipitation.

3.4. Effects of adsorptive mortar on performance of aggregates

3.4.1. Adsorption capacity of aggregates coated with adsorptive mortar

When the adsorptive aggregate is coated with different adsorptive mortar, the adsorption capacity with different initial P concentration is presented in Fig. 12. The adsorptive aggregate is immersed in P-solution with an initial concentration of 1215.3 mg/L, 1849.3 mg/L and 2967.5 mg/L, the adsorption capacity of the adsorptive aggregate particle coated with normal mortar (P-C0) is decreased by 18.2%, 24.7% and 48.4%, respectively, compared to the adsorptive aggregate (SS75) without coating.

The results also show that the porous adsorptive mortar significantly improves the adsorption capacity of the adsorptive aggregate, compared to the P-C0. When the P-concentration is 1215.3 mg/L, 1849.3 mg/L and 2967.5 mg/L, the P-adsorption capacity of the adsorptive mortar is 11.0–13.5 mg/g, 12.75–18.0 mg/g and 11.5–16.5 mg/g, respectively, and the P-removal rate is 35.9–44.4%, 39.3–27.6%, 22.1–15.4%, respectively. Compared to previous studies, the adsorption capacity is significantly higher than that of most pervious concrete, bio-based materials and industrial by-products. In this study, the P-HM1 shows the highest adsorption capacity and removal rate for the mortar-coated adsorptive aggregates, and its adsorption capacity increases by 20.0%, 24.1% and 34.7%, respectively, with an initial P-concentration of 1215.3 mg/L, 1849.3 mg/L and 2967.5 mg/L, com-

pared to the P-C0. The increase in the adsorption capacity of the mortar-coated adsorptive aggregate is mainly attributed to the increase of the micropores and permeability. In addition, when the addition of the SS is 10%, the mortar-coated adsorptive aggregate shows good adsorption capacity regardless of the initial concentration. Considering a balance between mechanical strength and adsorption capacity, the HM with a dosage of 0.5 wt% and the SS with a dosage of 10 wt% are recommended for the adsorptive mortar.

3.4.2. Adsorption mechanism of adsorptive aggregates

Previous studies have shown that physical and chemical methods can usually be used to increase the adsorption capacity of adsorptive materials. Physical methods such as increasing the amount of micropores, connectivity or specific surface area [22], and chemical methods such as to increase the leaching of Ca^{2+} ion for promoting its binding to phosphate and the formation of P-Ca precipitation are often utilized [29]. In this study, the physical and chemical methods are applied for improving the adsorption performance of cement-coasted adsorptive aggregates, respectively. The porous HM is applied to improve the porosity and permeability of adsorptive mortar for increasing the leaching of Ca^{2+} ion by the physical method. The SS is applied to further increase the adsorption capacity of the mortar-coated adsorptive aggregate by the chemical adsorption.

The schematic diagram of the adsorption process and mechanism of mortar-coated adsorptive aggregates for P-removal is shown in Fig. 13. The conventional aggregate is coated by the conventional mortar, most of the PO_4-P can not be in contact with the conventional aggregate (Fig. 13a). More importantly, conventional aggregates do not have the adsorption capacity, thereby a small amount of the PO_4-P can be adsorbed by the Ca^{2+} ion leached from the conventional mortar, which explains the low P-removal capacity of conventional porous concrete.

However, for adsorptive aggregate coated with conventional mortar, due to the high adsorption capacity of the adsorptive aggregate (SS75), as shown in Fig. 12, as long as the PO_4-P can penetrate the coating layer of the conventional mortar, it can be adsorbed by the adsorptive aggregate and mortar. It has to be noted that still only a small amount of PO_4-P can be in contact with the adsorptive aggregate because of the highly dense structure of the conventional mortar (Fig. 13b).

When the adsorptive aggregate is coated by the porous adsorptive mortar, due to the increase in the adsorption capacity and permeability of the adsorptive mortar, more PO_4-P can penetrate the coating layer and contact with the adsorptive aggregate, and finally, be absorbed by the internal adsorptive aggregate and the external adsorptive mortar layer (Fig. 13c).

4. Conclusions

In this study, to improve the adsorption performance of the adsorptive concrete for phosphorus (P) removal from stormwater runoff, a porous permeable mortar with good permeability and adsorption is proposed. The chemical and physical methods by adding adsorptive materials (steel slag (SS)) and porous materials (heat-treated miscanthus (HM)), respectively, are used to increase the adsorption capacity of the cement mortar. The effects of the SS and the HM powder on cement hydration are analyzed. The physical, mechanical properties and adsorption characteristics of adsorptive mortar and its effects on adsorption performance of the aggregate are investigated. The following conclusions can be drawn based on the acquired results:

(1) The HM (0.5 wt% and 1 wt%) shows an insignificant effect on cement hydration thanks to the pyrolysis of oxygen-containing saccharides. The SS (5 wt% and 10 wt%) slightly reduces the total heat of cement hydration by 3.4–6.8%.

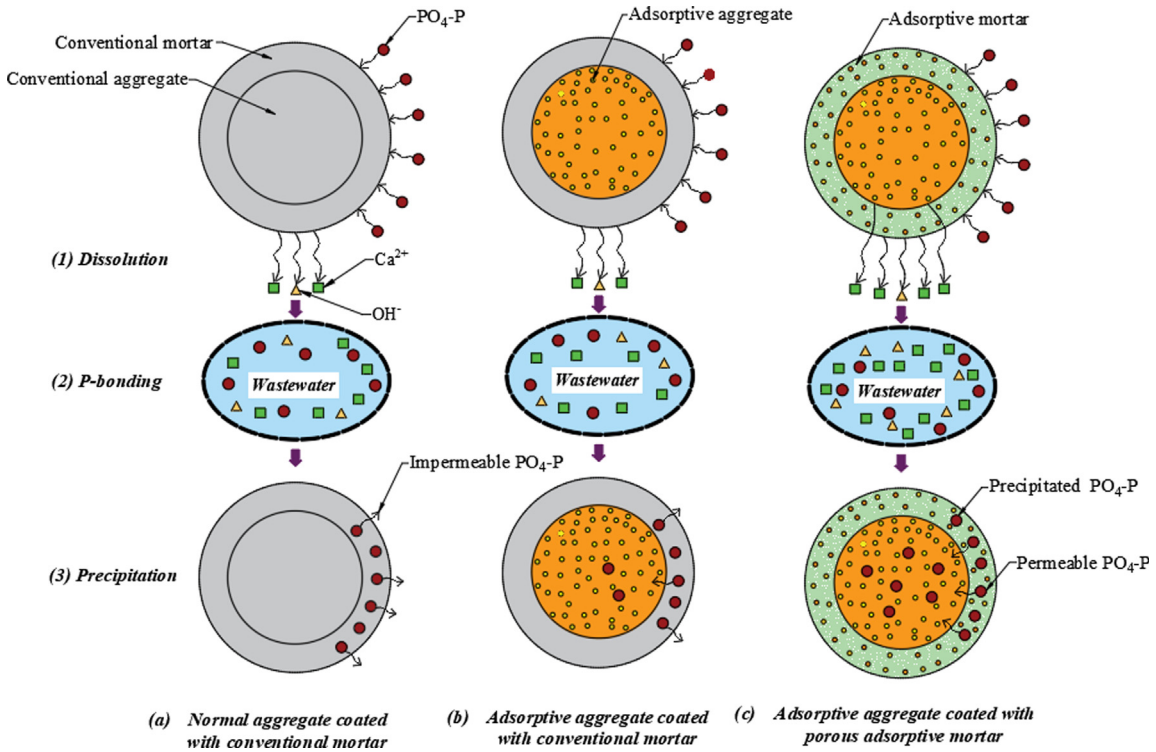

Fig. 13. Schematic diagram of the adsorption process and mechanism of adsorptive aggregates coated with porous adsorptive mortar for P-removal.

(2) The HM slightly decreases the density of adsorptive mortar (up to 3.1%), while the SS significantly increases the density (up to 8.0%). The HM can be applied to improve the permeability of the adsorptive mortar (up to 10.0%). However, a high content of the HM ($\geq$1 wt%) would result in significant decrease in mechanical strength.
(3) High adsorption capacity of the adsorptive mortar is observed, namely 30.4 mg/g, 46.2 mg/g and 74.2 mg/g, with a corresponding initial P-concentration of 1215.3 mg/L, 1849.3 mg/L and 2967.5 mg/L. The mortar-coated aggregate (P-HM1) shows the highest adsorption capacity and removal rate for P-removal, with an increase of 20.0–34.7%, compared to the P-C0. The Ca^{2+} leached from the mortar and the SS is one of the main metal ions for the formation of Ca-P precipitates in solution. Besides, the increase in the micropores of the adsorptive mortar by the porous HM contributes to the physical adsorption.
(4) The porous HM and the SS can significantly improve the adsorption performance of the mortar-coated aggregate by increasing the permeability and the release of Ca^{2+} ion. The HM with a dosage of 0.5 wt% and the SS with a dosage of 10.0 wt% are recommended for the adsorptive mortar, without obvious sacrifices on other properties.

CRediT authorship contribution statement

Fan Wu: Methodology, Investigation, Data curation, Formal analysis, Validation, Writing - original draft. **Qingliang Yu:** Conceptualization, Supervision, Project administration, Writing - review & editing. **H.J.H. Brouwers:** Supervision, Writing - review & editing.

Declaration of Competing Interest

The authors declare that they have no known competing financial interests or personal relationships that could have appeared to influence the work reported in this paper.

Acknowledgements

This work was funded by China Scholarship Council (CSC) Fund (Grant No. 201806240037), the Special Research Associate Project of Chinese Academy of Sciences (E1K2180), Institute of Mountain Hazards and Environment (Chengdu) and Eindhoven University of Technology. The authors gratefully thank Ing. Anneke Delsing for the chemical test and analysis, Mr. J.G. van Gilst from Vibers (The Netherlands), Dr. P. Spiesz from ENCI (The Netherlands) and Prof. Dr. S.R. van der Laan from TATA Steel (The Netherlands) for the materials supply.

References

[1] M. Gizińska-Górna, K. Jóźwiakowski, M. Marzec, A. Pytka, Analysis of the influence of a hybrid constructed wetland wastewater treatment plant on the water quality of the receiver, Annu. Set Environ. Prot. 19 (2017) 370–393.
[2] R.T. Bannerman, D.W. Owens, R.B. Dodds, N.J. Hornewer, Sources of pollutants in Wisconsin stormwater, Water Sci. Technol. 28 (1993) 241–259.
[3] T. Park, V. Ampunan, S. Maeng, E. Chung, Application of steel slag coated with sodium hydroxide to enhance precipitation-coagulation for phosphorus removal, Chemosphere 167 (2017) 91–97, https://doi.org/10.1016/j.chemosphere.2016.09.150.
[4] G. Li, S. Gao, G. Zhang, X. Zhang, Enhanced adsorption of phosphate from aqueous solution by nanostructured iron(III)-copper(II) binary oxides, Chem. Eng. J. 235 (2014) 124–131, https://doi.org/10.1016/j.cej.2013.09.021.
[5] M.M. Mekonnen, A.Y. Hoekstra, Global anthropogenic phosphorus loads to freshwater and associated grey water footprints and water pollution levels: a high-resolution global study, Water Resour. Res. 54 (2018) 345–358, https://doi.org/10.1002/2017WR020448.
[6] N.I. Vázquez-Rivera, L. Soto-Pérez, J.N. St John, O.I. Molina-Bas, S.S. Hwang, Optimization of pervious concrete containing fly ash and iron oxide nanoparticles and its application for phosphorus removal, Constr. Build. Mater. 93 (2015) 22–28, https://doi.org/10.1016/j.conbuildmat.2015.05.110.
[7] A.N. Shabalala, S.O. Ekolu, S. Diop, F. Solomon, Pervious concrete reactive barrier for removal of heavy metals from acid mine drainage – column study, J. Hazard. Mater. 323 (2017) 641–653, https://doi.org/10.1016/j.jhazmat.2016.10.027.
[8] M. Jo, L. Soto, M. Arocho, J. St John, S. Hwang, Optimum mix design of fly ash geopolymer paste and its use in pervious concrete for removal of fecal coliforms and phosphorus in water, Constr. Build. Mater. 93 (2015) 1097–1104, https://doi.org/10.1016/j.conbuildmat.2015.05.034.
[9] K. Okano, M. Uemoto, J. Kagami, K. Miura, T. Aketo, M. Toda, K. Honda, H. Ohtake, Novel technique for phosphorus recovery from aqueous solutions using amorphous calcium silicate hydrates (A-CSHs), Water Res. 47 (2013) 2251–2259, https://doi.org/10.1016/j.watres.2013.01.052.
[10] F. Wu, Q. Yu, C. Liu, H.J.H. Brouwers, L. Wang, Effect of surface treatment of apricot shell on the performance of lightweight bio-concrete, Constr. Build. Mater. 229 (2019) 116859, https://doi.org/10.1016/j.conbuildmat.2019.116859.
[11] J.P. Gustafsson, A. Renman, G. Renman, K. Poll, Phosphate removal by mineral-based sorbents used in filters for small-scale wastewater treatment, Water Res. 42 (2008) 189–197, https://doi.org/10.1016/j.watres.2007.06.058.
[12] N.M. Agyei, C.A. Strydom, J.H. Potgieter, The removal of phosphate ions from aqueous solution by fly ash, slag, ordinary Portland cement and related blends, Cem. Concr. Res. 32 (2002) 1889–1897, https://doi.org/10.1016/S0008-8846(02)00888-8.
[13] S. De Carvalho Gomes, J.L. Zhou, W. Li, G. Long, Progress in manufacture and properties of construction materials incorporating water treatment sludge: a review, Resour. Conserv. Recycl. 145 (2019) 148–159, https://doi.org/10.1016/j.resconrec.2019.02.032.
[14] C. Barca, C. Gérente, D. Meyer, F. Chazarenc, Y. Andrès, Phosphate removal from synthetic and real wastewater using steel slags produced in Europe, Water Res. 46 (2012) 2376–2384, https://doi.org/10.1016/j.watres.2012.02.012.
[15] C. Shi, Steel slag - its production, processing, characteristics, and cementitious properties, J. Mater. Civ. Eng. 16 (2004) 230–236, https://doi.org/10.1061/(ASCE)0899-1561(2004)16:3(230).
[16] L.I. Bowden, A.P. Jarvis, P.L. Younger, K.L. Johnson, Phosphorus removal from waste waters using basic oxygen steel slag, Environ. Sci. Technol. 43 (2009) 2476–2481, https://doi.org/10.1021/es801626d.
[17] S. Kourounis, S. Tsivilis, P.E. Tsakiridis, G.D. Papadimitriou, Z. Tsibouki, Properties and hydration of blended cements with steelmaking slag, Cem. Concr. Res. 37 (2007) 815–822, https://doi.org/10.1016/j.cemconres.2007.03.008.
[18] F. Han, Z. Zhang, D. Wang, P. Yan, Hydration heat evolution and kinetics of blended cement containing steel slag at different temperatures, Thermochim. Acta 605 (2015) 43–51, https://doi.org/10.1016/j.tca.2015.02.018.
[19] J. Li, Q. Yu, J. Wei, T. Zhang, Structural characteristics and hydration kinetics of modified steel slag, Cem. Concr. Res. 41 (2011) 324–329, https://doi.org/10.1016/j.cemconres.2010.11.018.
[20] T.A. Kua, M.A. Imteaz, A. Arulrajah, S. Horpibulsuk, Environmental and economic viability of Alkali Activated Material (AAM) comprising slag, fly ash and spent coffee ground, Int. J. Sustain. Eng. 12 (2019) 223–232, https://doi.org/10.1080/19397038.2018.1492043.
[21] F. Wu, Q. Yu, F. Gauvin, H.J.H. Brouwers, A facile manufacture of highly adsorptive aggregates using steel slag and porous expanded silica for phosphorus removal, Resour. Conserv. Recycl. (2021) 105238, https://doi.org/10.1016/j.resconrec.2020.105238.
[22] C. Jiang, L. Jia, B. Zhang, Y. He, G. Kirumba, Comparison of quartz sand, anthracite, shale and biological ceramsite for adsorptive removal of phosphorus from aqueous solution, J. Environ. Sci. (China) 26 (2014) 466–477, https://doi.org/10.1016/S1001-0742(13)60410-6.
[23] Y. Zhang, G. Li, Principle and application of activated carbon-nanofiltration in treatment of Mmicro-polluted source water, Science Press, Beijing, 2011.
[24] J. Clifton-Brown, A. Hastings, M. Mos, Progress in upscaling Miscanthus biomass production for the European bio-economy with seed-based hybrids, GCB Bioenergy 9 (2017) 6–17, https://doi.org/10.1111/gcbb.12357.
[25] Y. Chen, F. Wu, Q. Yu, H.J.H. (Jos) Brouwers, Bio-based ultra-lightweight concrete applying Miscanthus fibers: acoustic absorption and thermal insulation, Cem. Concr. Compos. 114 (2020) 103829.
[26] Y. Chen, Q.L. Yu, H.J.H. Brouwers, Acoustic performance and microstructural analysis of bio-based lightweight concrete containing miscanthus, Constr. Build. Mater. 157 (2017) 839–851, https://doi.org/10.1016/j.conbuildmat.2017.09.161.
[27] K. Hosni, S. Ben Moussa, A. Chachi, M. Ben Amor, The removal of PO43- by calcium hydroxide from synthetic wastewater: optimisation of the operating conditions, Desalination 223 (2008) 337–343, https://doi.org/10.1016/j.desal.2007.01.213.
[28] N. Bellier, F. Chazarenc, Y. Comeau, Phosphorus removal from wastewater by mineral apatite, Water Res. 40 (2006) 2965–2971, https://doi.org/10.1016/j.watres.2006.05.016.
[29] F. Wu, Q. Yu, F. Gauvin, H.J.H. Brouwers, C. Liu, Phosphorus removal from aqueous solutions by adsorptive concrete aggregates, J. Clean. Prod. 278 (2021) 123933, https://doi.org/10.1016/j.jclepro.2020.123933.

[30] J. Hao, H. Tian, Z. Hu, Co-pyrolysis characteristics of miscanthus corn stalks and lignite, Coal Convers. 42 (2019) 22–30.
[31] Q. Wang, P. Yan, Hydration properties of basic oxygen furnace steel slag, Constr. Build. Mater. 24 (2010) 1134–1140, https://doi.org/10.1016/j.conbuildmat.2009.12.028.
[32] C. Barca, D. Meyer, M. Liira, P. Drissen, Y. Comeau, Y. Andrès, F. Chazarenc, Steel slag filters to upgrade phosphorus removal in small wastewater treatment plants: removal mechanisms and performance, Ecol. Eng. 68 (2014) 214–222, https://doi.org/10.1016/j.ecoleng.2014.03.065.
[33] S. Zhuang, Q. Wang, Inhibition mechanisms of steel slag on the early-age hydration of cement, Cem. Concr. Res. 140 (2021) 106283, https://doi.org/10.1016/j.cemconres.2020.106283.
[34] K. Kochova, K. Schollbach, F. Gauvin, H.J.H. Brouwers, Effect of saccharides on the hydration of ordinary Portland cement, Constr. Build. Mater. 150 (2017) 268–275, https://doi.org/10.1016/j.conbuildmat.2017.05.149.
[35] H. Yin, Y. Yun, Y. Zhang, C. Fan, Phosphate removal from wastewaters by a naturally occurring, calcium-rich sepiolite, J. Hazard. Mater. 198 (2011) 362–369, https://doi.org/10.1016/j.jhazmat.2011.10.072.
[36] E. Boix, E. Gineau, O. Joan, G. Mouille, P. Navard, Influence of chemical treatments of miscanthus stem fragments on polysaccharide release in the presence of cement and on the mechanical properties of bio-based concrete materials, Cem. Concr. Compos. 105 (2020) 1–8, https://doi.org/10.1016/j.cemconcomp.2019.103429.
[37] G.C.H. Doudart de la Grée, Q.L. Yu, H.J.H. Brouwers, Assessing the effect of CaSO4 content on the hydration kinetics, microstructure and mechanical properties of cements containing sugars, Constr. Build. Mater. 143 (2017) 48–60, https://doi.org/10.1016/j.conbuildmat.2017.03.067.
[38] T. Le Ngoc Huyen, M. Queneudec T'Kint, C. Remond, B. Chabbert, R.M. Dheilly, Saccharification of Miscanthus x giganteus, incorporation of lignocellulosic by-product in cementitious matrix, Comptes Rendus - Biol. 334 (2011) 837.e1–837.e11. https://doi.org/10.1016/j.crvi.2011.07.008.
[39] X. Ma, X. Hao, X. Chen, Z. Gao, chao D. Wei, B. Zhou, Study on biochar properties analysis with scanning electron microscope-energy dispersive X-ray spectroscopy (SEM-EDX), Spectrosc. Spectr. Anal. 36 (2016) 1670–1673.
[40] G. Liu, K. Schollbach, S. van der Laan, P. Tang, M.V.A. Florea, H.J.H. Brouwers, Recycling and utilization of high volume converter steel slag into CO2 activated mortars – the role of slag particle size, Resour. Conserv. Recycl. 160 (2020) 104883, https://doi.org/10.1016/j.resconrec.2020.104883.
[41] Y. Ling, K. Wang, W. Li, G. Shi, P. Lu, Effect of slag on the mechanical properties and bond strength of fly ash-based engineered geopolymer composites, Compos. Part B Eng. 164 (2019) 747–757, https://doi.org/10.1016/j.compositesb.2019.01.092.
[42] S.D.C. Gomes, J.L. Zhou, W. Li, F. Qu, Recycling of raw water treatment sludge in cementitious composites: effects on heat evolution, compressive strength and microstructure, Resour. Conserv. Recycl. 161 (2020) 104970, https://doi.org/10.1016/j.resconrec.2020.104970.
[43] F. Wu, C. Liu, W. Sun, Y. Ma, L. Zhang, Effect of peach shell as lightweight aggregate on mechanics and creep properties of concrete, Eur. J. Environ. Civ. Eng. (2019) 1–21, https://doi.org/10.1080/19648189.2018.1515667.
[44] P. Shafigh, H. Mahmud, M.Z. Jumaat, Effect of steel fiber on the mechanical properties of oil palm shell lightweight concrete, Mater. Des. 32 (2011) 3926–3932, https://doi.org/10.1016/j.matdes.2011.02.055.
[45] A. Akkaoui, S. Caré, M. Vandamme, Experimental and micromechanical analysis of the elastic properties of wood-aggregate concrete, Constr. Build. Mater. 134 (2017) 346–357, https://doi.org/10.1016/j.conbuildmat.2016.12.084.
[46] F. Wu, C. Liu, L. Zhang, Y. Lu, Y. Ma, Comparative study of carbonized peach shell and carbonized apricot shell to improve the performance of lightweight concrete, Constr. Build. Mater. 188 (2018) 758–771, https://doi.org/10.1016/j.conbuildmat.2018.08.094.
[47] P. Shafigh, H. Ghafari, H. Bin Mahmud, M.Z. Jumaat, A comparison study of the mechanical properties and drying shrinkage of oil palm shell and expanded clay lightweight aggregate concretes, Mater. Des. 60 (2014) 320–327, https://doi.org/10.1016/j.matdes.2014.04.001.
[48] M. Bederina, M. Gotteicha, B. Belhadj, R.M. Dheily, M.M. Khenfer, M. Queneudec, Drying shrinkage studies of wood sand concrete - effect of different wood treatments, Constr. Build. Mater. 36 (2012) 1066–1075, https://doi.org/10.1016/j.conbuildmat.2012.06.010.
[49] K. Ghavami, Bamboo as reinforcement in structural concrete elements, Cem. Concr. Compos. 27 (2005) 637–649, https://doi.org/10.1016/j.cemconcomp.2004.06.002.
[50] Y. Luo, L. Zhao, H. Meng, X. Xiang, X. Zhao, G. Li, Q. Lin, Physio-chemical characterization of biochars pyrolyzed from miscanthus under two different temperatures, Trans. Chinese Soc. Agric. Eng. 29 (2013) 208–217.
[51] Y. Han, S. Park, C. Lee, J. Park, N. Choi, S. Kim, Phosphate removal from aqueoussolution by aluminum (Hydr)oxide-coated sand, Environ. Eng. Res. 14 (2009) 164–169.
[52] J.H. Park, J.J. Wang, S.H. Kim, J.S. Cho, S.W. Kang, R.D. Delaune, D.C. Seo, Phosphate removal in constructed wetland with rapid cooled basic oxygen furnace slag, Chem. Eng. J. 327 (2017) 713–724, https://doi.org/10.1016/j.cej.2017.06.155.
[53] A. Drizo, C.A. Frost, J. Grace, K.A. Smith, Physico-chemical screening of phosphate-removing substrates for use in constructed wetland systems, Water Res. 33 (1999) 3595–3602, https://doi.org/10.1016/S0043-1354(99)00082-2.
[54] F. Gan, J. Zhou, H. Wang, C. Du, X. Chen, Removal of phosphate from aqueous solution by thermally treated natural palygorskite, Water Res. 43 (2009) 2907–2915, https://doi.org/10.1016/j.watres.2009.03.051.
[55] K.W. Jung, M.J. Hwang, K.H. Ahn, Y.S. Ok, Kinetic study on phosphate removal from aqueous solution by biochar derived from peanut shell as renewable adsorptive media, Int. J. Environ. Sci. Technol. 12 (2015) 3363–3372, https://doi.org/10.1007/s13762-015-0766-5.
[56] S. Ramola, T. Mishra, G. Rana, R.K. Srivastava, Characterization and pollutant removal efficiency of biochar derived from baggase, bamboo and tyre, Environ. Monit. Assess. 186 (2014) 9023–9039, https://doi.org/10.1007/s10661-014-4062-5.
[57] J.S. Han, S.H. Min, Y.K. Kim, Removal of phosphorus using AMD-treated lignocellulosic material, For. Prod. J. 55 (2005) 48–53.
[58] X. Tan, Y. Liu, G. Zeng, X. Wang, X. Hu, Y. Gu, Z. Yang, Application of biochar for the removal of pollutants from aqueous solutions, Chemosphere 125 (2015) 70–85, https://doi.org/10.1016/j.chemosphere.2014.12.058.
[59] K.R. Helyar, D.N. Munns, R.G. Burau, Adsorption of phosphate by gibbsite I. Effects of neutral chloride salts of calcium, magnesium, sodium, and potassium, J. Soil Sci. 27 (1976) 307–314.
[60] K.R. Helyar, D.N. Munns, R.G. Burau, Adsorption of phosphate by gibbsite II. Formation of a surface complex involving divalent cations, J. Soil Sci. 27 (1976) 315–323.
[61] Q. Wang, M. Shi, J. Yang, Influence of classified steel slag with particle sizes smaller than 20 μm on the properties of cement and concrete, Constr. Build. Mater. 123 (2016) 601–610, https://doi.org/10.1016/j.conbuildmat.2016.07.042.
[62] N. Sazonova, N. Skripnikova, Physico-mechanical and physico-chemical properties of synthesized cement based on plasma-and wet technologies, AIP Conf. Proc. 1698 (2016), https://doi.org/10.1063/1.4937888.
[63] A.N. Christensen, T.R. Jensen, J.C. Hanson, Formation of ettringite, Ca6Al2(SO4)3(OH)12·26H2O, AFt, and monosulfate, Ca4Al2O6(SO4)·14H2O, AFm-14, in hydrothermal hydration of Portland cement and of calcium aluminum oxide - calcium sulfate dihydrate mixtures studied by in situ synchrotron X-ray pow, J. Solid State Chem. 177 (2004) 1944–1951, https://doi.org/10.1016/j.jssc.2003.12.030.
[64] R. Ylmén, U. Jäglid, B.M. Steenari, I. Panas, Early hydration and setting of Portland cement monitored by IR, SEM and Vicat techniques, Cem. Concr. Res. 39 (2009) 433–439, https://doi.org/10.1016/j.cemconres.2009.01.017.
[65] B. Yilmaz, A. Olgun, Studies on cement and mortar containing low-calcium fly ash, limestone, and dolomitic limestone, Cem. Concr. Compos. 30 (2008) 194–201, https://doi.org/10.1016/j.cemconcomp.2007.07.002.
[66] D. Vaičiukynienė, G. Skripkiūnas, M. Daukšys, V. Sasnauskas, Cement hydration with zeolite-based additive, Chemija 24 (2013) 271–278.
[67] M.A. Trezza, A.E. Lavat, Analysis of the system 3CaO·Al2O3-CaSO4· 2H2O-CaCO3-H2O by FT-IR spectroscopy, Cem. Concr. Res. 31 (2001) 869–872, https://doi.org/10.1016/S0008-8846(01)00502-6.
[68] I. García Lodeiro, D.E. Macphee, A. Palomo, A. Fernández-Jiménez, Effect of alkalis on fresh C-S-H gels. FTIR analysis, Cem. Concr. Res. 39 (2009) 147–153, https://doi.org/10.1016/j.cemconres.2009.01.003.
[69] M.A.M. Ariffin, M.A.R. Bhutta, M.W. Hussin, M. Mohd Tahir, N. Aziah, Sulfuric acid resistance of blended ash geopolymer concrete, Constr. Build. Mater. 43 (2013) 80–86, https://doi.org/10.1016/j.conbuildmat.2013.01.018.
[70] R.J. Galán-Arboledas, J. Álvarez de Diego, M. Dondi, S. Bueno, Energy, environmental and technical assessment for the incorporation of EAF stainless steel slag in ceramic building materials, J. Clean. Prod. 142 (2017) 1778–1788, https://doi.org/10.1016/j.jclepro.2016.11.110.
[71] S. Duan, H. Liao, F. Cheng, H. Song, H. Yang, Investigation into the synergistic effects in hydrated gelling systems containing fly ash, desulfurization gypsum and steel slag, Constr. Build. Mater. 187 (2018) 1113–1120, https://doi.org/10.1016/j.conbuildmat.2018.07.241.
[72] C.F. Chang, J.W. Chen, The experimental investigation of concrete carbonation depth, Cem. Concr. Res. 36 (2006) 1760–1767, https://doi.org/10.1016/j.cemconres.2004.07.025.
[73] A. Kaasik, C. Vohla, R. Mõtlep, Ü. Mander, K. Kirsimäe, Hydrated calcareous oil-shale ash as potential filter media for phosphorus removal in constructed wetlands, Water Res. 42 (2008) 1315–1323, https://doi.org/10.1016/j.watres.2007.10.002.